

**SEASONAL AND SPATIAL VARIABILITY OF OZONE AS INFERRED FROM MARCI UV DATA.** R.M. Haberle<sup>1</sup>, C. Pilorget<sup>2</sup>, M. Wolff<sup>3</sup>, F. Lefevre<sup>4</sup>, and F. Forget<sup>5</sup>. <sup>1</sup>Space Science Division, NASA/Ames Research Center, Moffett Field CA, 94035, <sup>2</sup>Institut Supérieur de l'Aéronautique et de l'Espace, 10, avenue Edouard-Belin - BP 54032 - 31055 Toulouse CEDEX 4 - France, <sup>3</sup>Space Science Institute, 4750 Walnut Street, Suite 205, Boulder, CO 80301, <sup>4</sup>UPMC Univ Paris 06, Service d'Aéronomie, Paris, F-75005 France, <sup>5</sup>UPMC Univ Paris 06, Laboratoire de Meteorologie Dynamique, Paris F-75005.

**Introduction:** The Mars Reconnaissance Orbiter (MRO) has been operating at Mars for almost a full Mars year. The Mars Color Imager (MARCI) on board MRO is a wide-angle push frame camera that has 7 color bands: 5 in the visible and 2 in the UV. The low altitude (~300 km), high inclination (~92°), near-circular orbit of MRO permits the acquisition of limb-to-limb views along the entire pole-to-pole ground track of the 3PM sunlit side on every orbit with substantial overlap in the polar regions. At nadir, MARCI typically acquires its data at ~1 km/pixel resolution in the visible, and ~10 km/pixel resolution in the UV.

The two UV channels are centered at 260 nm and 320 nm, and are referred to as Band-6 and Band-7 respectively. Band 6, which has a band pass of ~60 nm, is centered on the Hartley ozone (O<sub>3</sub>) absorption band, while Band-7, which has a band pass of ~50 nm, has negligible ozone absorption. Both bands are sensitive to the presence clouds and surface frost, but Band-6 is additionally affected by the presence of O<sub>3</sub>. To the extent the scattering properties of any aerosols present in the atmosphere are similar in each band, the ratio of the observed reflectances of Band-6 to Band-7, "B6/B7", serves as a proxy for the presence of O<sub>3</sub>. In general, where B6/B7~1, there is little O<sub>3</sub> absorption; where this ratio is depressed (B6/B7<1), O<sub>3</sub> is present. The exception to this general rule is over high elevations, such as the tops of volcanoes, where the surface pressure is low and Rayleigh scattering selectively reduces the Band-6 reflectance compared to Band-7. Clouds and dust also affect band reflectances. Obviously, full-up radiative transfer calculations are needed to account for these effects in order to retrieve absolute abundances, and such efforts are underway by the MARCI team.

However, in this paper we use the MARCI B6/B7 ratios to qualitatively estimate the seasonal and spatial variations of column ozone abundances, and we compare these patterns to those simulated by the LMD photochemical model of Lefevre et al. [1]. From these comparisons we gain insight into atmospheric mixing processes. We also use the B6/B7 ratios to infer dynamical properties of the polar atmosphere, which are also related to atmospheric mixing and transport.

We present data acquired from the beginning of the primary science phase P01 (which began on Nov. 8, 2006 at Ls=132.2°) through the end of P21 (which ended on July 31, 2008 at Ls=106.4°). Thus, these data span almost a full Mars year. As proxies for O<sub>3</sub>, the B6/B7 ratios are useful indicators of atmospheric dynamics because the lifetime of O<sub>3</sub>, which ranges from

hours at low latitudes to days at high latitudes, is commensurate with the time scale of large-scale baroclinic eddies.

**Data Analysis:** The raw spacecraft data are first sorted into their respective bands. The band data are then calibrated and map-projected into polar stereographic images with emission angles constrained to be less than 70°. At this stage the data consists of individual strips ~1500 km wide centered on a longitude dictated by the spacecraft's orbit. In general 12-13 such strips, which are obtained in a single Sol, cover the full 360° on longitude. However, gaps in longitude, which increase with decreasing latitude (see, for example, Figures 4 and 5 below), will exist because of our emission angle constraint and the low altitude of the spacecraft. We therefore chose to construct equator-to-pole, polar stereographic mosaics of the B6/B7 ratio for each hemisphere from 50 consecutive image strips, which corresponds to a period of time of about 4-5 sols (1.6-2.6° of Ls). These mosaics form part of the basis of our analysis, an example of which is shown in Fig. 1.

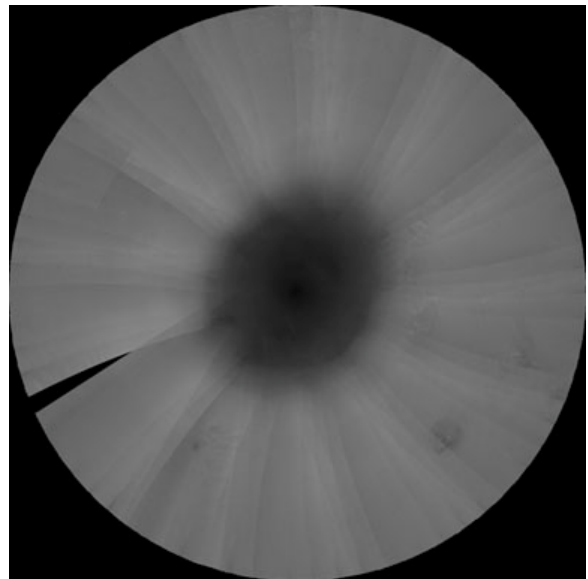


**Figure 1.** A north polar mosaic of 50 strips of MARCI B6/B7 ratios from Ls=3.7° to 5.7°. Note that most, but not all, of the longitudinal gaps have been eliminated.

**Results:** We begin by constructing zonal means. This is done by binning the mosaiced data into  $1^\circ$  latitude strips, forming the zonal mean, and contouring the results as a function of latitude and  $L_s$ . The result is shown in Fig. 2. In general the MARCI data indicate low column  $O_3$  abundances at low latitudes for all seasons. At high latitudes,  $O_3$  exhibits a distinct seasonal cycle, forming during the fall and winter seasons, and disappearing during the spring and summer. Peak abundances, as inferred from these ratios, appear to be higher in the north compared to the south. Furthermore, peak abundances in the north occur near spring equinox and linger well into mid spring, whereas peak abundances in the south occur during mid fall.

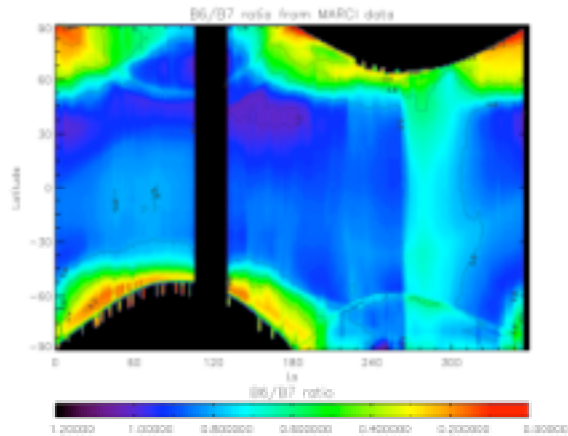


**Figure 2.** Zonal mean MARCI B6/B7 ratios. The vertical black bar centered at  $L_s=120^\circ$  represents a time period not yet sampled by MARCI. The blacked out regions at both poles represent the polar night where MARCI cannot observe. The thin arced features at high summer latitudes in both hemispheres are artifacts of our processing scheme. The abrupt decline in B6/B7 ratios at all latitudes commencing at  $L_s=260^\circ$  marks the onset of a global dust storm and does not represent and increase in  $O_3$  columns. Contour intervals are 0.2.

We compare these patterns with the LMD model in Fig. 3. Note that while the color schemes in Figs. 2 and 3 are similar, Fig. 2 is a band ratio while Fig. 3 is a column  $O_3$  abundance. As in the MARCI data, the LMD model shows low  $O_3$  columns at low latitudes throughout the year, and high fall/winter abundances at high latitudes in each hemisphere. Though there is a discernable low-latitude seasonal variation in the model, its magnitude is small ( $< 5 \mu\text{m-atm}$ ) and would be difficult to detect in the MARCI data. The major difference between MARCI and the LMD model in the regions where they overlap is the magnitude of the asymmetry in high latitude maxima. Zonal mean column  $O_3$  abundances peak around  $15 \mu\text{m-atm}$  in the south and  $40 \mu\text{m-atm}$  in the north. While we might expect depressed B6/B7 ratios in the south compared to the north because of elevation differences, the mag-

nitude of the decrease (about a factor of 3) needs to be carefully assessed with radiative transfer calculations to determine the reality of the simulated asymmetry. In any case, regardless of the magnitude of the asymmetry, it has implications for model mixing processes and can therefore provide constraints on tracer transport.

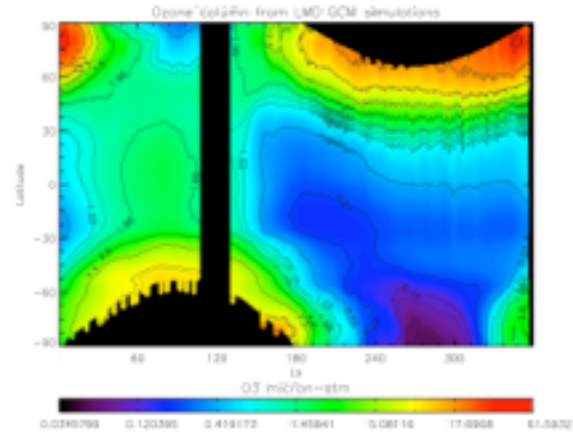


**Figure 3.** Zonal mean  $O_3$  columns as simulated by the LMD photochemical model of Lefevre et al. (2008). Units are  $\mu\text{m-atm}$ . The data are masked (blacked out regions) to facilitate comparison to the MARCI data.

MARCI data also show evidence for transient baroclinic wave activity in both hemispheres. Figures 4 and 5 show "snapshots" of the B6/B7 ratio at each pole during mid winter. In both instances there is evidence for a wave 3 feature distorting the polar vortex. In general the amplitude of these features, which vary between wave 3 and wave 2, is more pronounced in the north compared to the south. Furthermore, animations show these waves migrating eastward in each hemisphere as is expected for baroclinic waves.

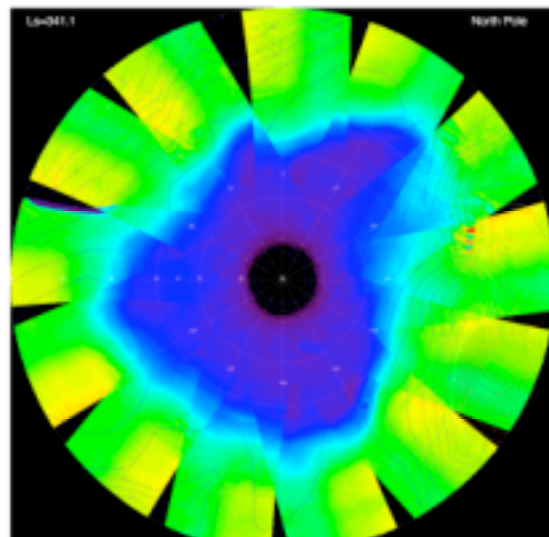


**Figure 4.** North polar projection (out to  $30^\circ\text{N}$ ) of the B6/B7 ratio based on 13 orbits at  $L_s=341.1^\circ$ . Ratios are presented in false color to bring out details. Blue regions are  $O_3$  rich, while green/yellow regions are  $O_3$  poor. Dotted contours represent topographic elevation in km.

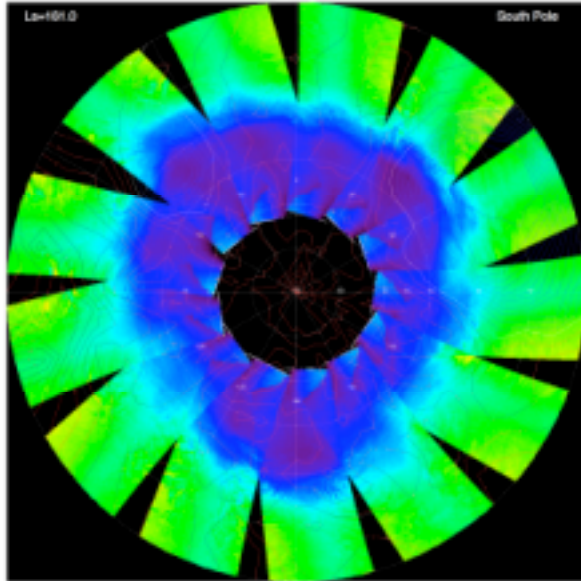


**Figure 5.** Same as Fig. 4, but for the southern hemisphere at  $L_s=161.0^\circ$ .

**Conclusions:** MARCI B6/B7 ratios are useful proxies for column  $O_3$ . The data suggest that  $O_3$  peaks at high latitudes during the fall/winter season in each hemisphere with similar magnitudes. The overall pattern seen by MARCI is very similar to that predicted by the LMD model, but differs from the model which shows a more pronounced hemispheric asymmetry in peak abundances. The reality of the simulated asymmetry can be addressed by comparing radiative transfer model calculations with the MARCI data.

**References:**

[1] Lefevre, F., et al. (2008) *Nature*, In press.